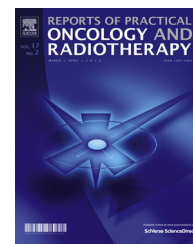




ELSEVIER

Available online at www.sciencedirect.com

ScienceDirect

journal homepage: <http://www.elsevier.com/locate/rpor>

Original research article

An empirical method for automatic determination of maximum number of segments in DMPO-based IMRT for Head and Neck cases

Vaitheeswaran Ranganathan^{a,b,*}, K. Joseph Maria Das^c^a Philips Radiation Oncology Systems, Philips India Ltd, Bangalore, India^b Research & Development Center, Bharathiar University, Coimbatore, India^c Department of Radiotherapy, Sanjay Gandhi Post Graduate Institute of Medical Sciences, Lucknow, India

ARTICLE INFO

Article history:

Received 11 February 2016

Received in revised form

15 May 2016

Accepted 8 September 2016

Keywords:

IMRT

Number of segments

Aperture-based IMRT

DMPO

Anatomy-guided segments

ABSTRACT

Aim: An empirical scheme called “anatomy-guided segment counting (AGSC)” is proposed for automatic selection of maximum number of segments (NOS) for direct machine parameter optimization (DMPO).

Background: Direct machine parameter optimization (DMPO) requires the user to define the maximum number of segments (NOS) in order to proceed with an optimization process. Till date there is no established approach to arrive at an optimal and case-specific maximum NOS in DMPO, and this step is largely left to the planner’s experience.

Materials and methods: The AGSC scheme basically uses the Beam’s-eye views (BEVs) and other planning parameters to decide on appropriate number of segments for the beam. The proposed algorithm was tested in eight H&N cases. We used Auto Plan feature available in Pinnacle3 (version 9.10.0) for driving the DMPO optimization.

Results: There is about 13% reduction in the composite objective value in AGSC plans as compared to the plans employing 6 NOS per beam and 10% increase in the composite objective value in AGSC plans as compared to the plans employing 8 NOS per beam. On the delivery efficiency front, there is about 10% increase in NOS in AGSC plans as compared to the plans employing 6 NOS per beam specification. Similarly, there is about 19% reduction in NOS in AGSC plans as compared to the plans employing 8 NOS per beam specification.

Conclusion: The study demonstrates that the AGSC method allows specifying appropriate number of segments into the DMPO module accounting for the complexity of a given case.

© 2016 Greater Poland Cancer Centre. Published by Elsevier Sp. z o.o. All rights reserved.

* Corresponding author at: Philips Radiation Oncology Systems, Philips India Ltd, Manyatha Tech Park, Nagavara, Bangalore 560045, India.
E-mail addresses: Vaitheeswaran.R@philips.com (V. Ranganathan), kjmariadas@hotmail.com (K.J. Maria Das).

<http://dx.doi.org/10.1016/j.rpor.2016.09.004>

1507-1367/© 2016 Greater Poland Cancer Centre. Published by Elsevier Sp. z o.o. All rights reserved.

1. Background

In inverse planning for IMRT, conversion of the fluence profiles into deliverable segments is an important step. The conversion is performed by a variety of algorithms, out of which aperture based optimization methods^{1–3} have become important and wide spread in clinical use. The advantage of aperture-based method is that the delivery constraints are directly incorporated in the inverse problem, which leads to the production of good quality plans with good deliverability. Direct machine parameter optimization (DMPO) is a commercial implementation of aperture-based optimization available in Pinnacle3 treatment planning system (TPS). With DMPO, MLC settings are produced directly within the optimization process. Therefore, there is no need for conversion, filtering or other kinds of post-processing, and there is no plan quality degradation.⁴ A detailed description of the DMPO algorithm has been discussed elsewhere.^{4,5} In general, DMPO results in considerably lesser number of segments and MUs as compared to the conventional two-step IMRT process, without any compromise in the plan quality.^{6–8}

DMPO requires the user to define the maximum number of segments (NOS) in order to proceed with the optimization process. If the maximum NOS defined by the user is too small, it can affect the plan optimality^{8,9}; conversely, if the maximum NOS is too large, it can directly impact the treatment efficiency. Many investigators have studied the impact of maximum NOS specification in DMPO plans and provided some recommendations.^{8–13} But till date, there is no established approach to arrive at an optimal and case-specific maximum NOS in DMPO, and this step is largely left to the planner's experience. Also in many instances, a suitable maximum NOS is found by a trial-and-error method, which is time consuming. Since DMPO optimizer invariably returns a plan with NOS close to the maximum number specified, specifying a number close to the optimal value is important in obtaining a good plan.

2. Aim

In this work, a novel and empirical scheme for automatic and case-specific selection of maximum NOS in DMPO-based IMRT is proposed. The scheme basically uses the segmented anatomic projections (SAPs) of the Planning Target Volume (PTV) and organs-at-risk (OARs) in the Beam's-eye-view (BEV) to determine the maximum NOS for each beam. Hence, the scheme can be regarded as "anatomy-guided segment counting (AGSC)" algorithm, the patent application of which can be found here.¹⁴

3. Materials and methods

3.1. Brief description of the algorithm

1. First, the AGSC algorithm takes as input the SAPs in the BEV to determine the areas of organs-at-risk (OAR) overlap with the composite target volume (i.e. the geometric sum of all PTVs).

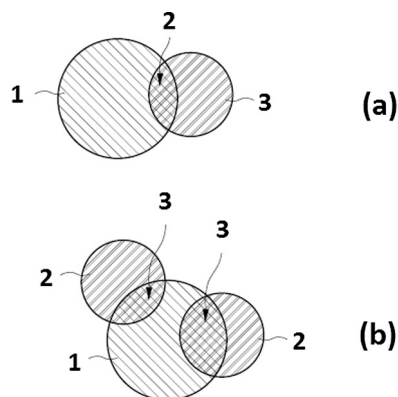


Fig. 1 – An illustration of different arrangement classes based on the segmented anatomic projections (SAPs) of the PTV and OAR and their overlaps in the Beam's-eye-view (BEV). (a) The arrangement of SAP 1 of PTV and SAP 3 of an OAR, which comprise a single overlapping region 2 (first arrangement class). (b) A further arrangement of SAP 1 of PTV and of SAP 2 of two OARs (second arrangement class).

Table 1 – A look-up table for the number of Boolean combinations (number of segments) for possible PTV-OAR overlaps based on arrangement class.

Number of OAR overlaps	Maximum NOS per beam		
	First arrangement class	Second arrangement class (before Boolean reduction)	Second arrangement class (after Boolean reduction)
0	1	Nil	Nil
1	3	Nil	Nil
2	Nil	6	3–6
3	Nil	9	6–8
4	Nil	12	8–11

2. Then, the number of regions overlapping with the composite target is counted and a combinatorial combination of these regions is derived from a set of Boolean combinations applicable to the segmented structures (Fig. 1 and Table 1).
3. The combination of sub-regions computed above along with other processes, such as segment pruning using minimum segment size (MSS) and Boolean reduction (BR) are used to arrive at the maximum NOS per beam.
4. The maximum NOS per beam obtained above is summed over all beams and the resulting total maximum NOS (per plan) is fed into the DMPO algorithm as a delivery constraint.
5. The DMPO algorithm uses AGSC-predicted maximum NOS and produces the optimal fluence along with deliverable segments.

3.2. Detailed description

3.2.1. Boolean combinations

The number of segments determination in the AGSC method is adapted to determine a number of regions of overlap between

the SAP of the composite target volume (hereafter referred to as PTV) and the SAP of one or more OARs in a given BEV. First, the AGSC algorithm takes as input the anatomical projections in the respective BEV image, in order to determine the areas of overlap. The number of regions overlapping with the PTV is counted and a combinatorial combination of these regions is computed. This can be computed from possible Boolean combinations applicable to a set of structures.

3.2.2. Arrangement class

The algorithm is further adapted to classify the arrangement of the SAPs of the PTV and of the OAR into a predefined arrangement class to determine the maximum NOS per beam, wherein the arrangement is classified depending on the number of overlaps of the PTV and OAR. Fig. 1a shows an arrangement of SAP 1 of PTV and SAP 3 of an OAR, which comprise a single overlapping region 2. Such an arrangement of the SAPs having a single overlapping region can be assigned to a first arrangement class. Fig. 1b shows a further arrangement of SAP 1 of PTV and of SAPs 2 of two OARs. This arrangement comprises two overlapping regions 3. Such an arrangement having more than one overlapping region can be assigned to a second arrangement class. For each arrangement of the SAPs of the PTV and OAR a combinatorial term can be determined, which describes the different overlapping and non-overlapping regions of the SAP of the PTV. For instance, for the arrangement shown in Fig. 1a, the following combinatorial term can be defined:

1. T ,
2. $T \cap O1$,
3. $T - \{T \cap O1\}$

wherein T indicates the SAP 1 of the PTV and $O1$ indicates the SAP 3 of the OAR shown in Fig. 1a. The combinatorial term for the arrangement shown in Fig. 1b can be defined by:

1. T ,
2. $T \cap O1$,
3. $T - \{T \cap O1\}$,
4. $T \cap O2$,
5. $T - \{T \cap O2\}$,
6. $T - \{T \cap O1\} - \{T \cap O2\}$

wherein the SAPs 2 of the OARs are represented by $O1$ and $O2$, respectively.

3.2.3. Minimum segment size (MSS)

MSS is an input to AGSC algorithm for determining maximum NOS. If the size of an overlapping region (e.g. $\{T \cap O2\}$) or a combinatorial term (e.g. $T - \{T \cap O1\} - \{T \cap O2\}$) is smaller than a predefined MSS value, the term is preferentially not counted, when determining the maximum NOS per beam. In AGSC approach, the MSS is generally set to be greater than 2 cm^2 to avoid dosimetric errors during treatment delivery.

3.2.4. Boolean reduction (BR)

As the number of OAR overlaps increases, the combinatorial terms involving overlapping segments are reduced. This process can be termed as “Boolean reduction (BR)”. This final step is done to exclude redundant and overlapping segments from segment counting process. Consider for instance a three OAR

overlap situation. The usual terms in such situations would be given by:

1. T ,
2. $T \cap O1$,
3. $T - \{T \cap O1\}$,
4. $T \cap O2$,
5. $T - \{T \cap O2\}$,
6. $T - \{T \cap O1\} - \{T \cap O2\}$
7. $T \cap O3$,
8. $T - \{T \cap O3\}$,
9. $T - \{T \cap O1\} - \{T \cap O2\} - \{T \cap O3\}$,

It is evident that the later terms 6, 8 and 9 introduce many overlapping segments and, hence, they are eliminated during the counting process. The removal of overlapping segments will be based on the composite size of all PTVs and the level of their overlap with OAR. Essentially, for lesser PTV-OAR overlaps and smaller PTVs, the number of segments getting excluded from counting through the BR process will be relatively larger; likewise, for higher PTV-OAR overlaps and bigger PTVs, the number of segments getting excluded from counting will be relatively smaller. To compute the number of segments getting excluded per BEV for a given case, we use Eq. (1) shown below:

$$NOS_{excluded}(\theta) = NOS_{excluded}^{Ref}(\theta) * \left[\frac{V_{PTV}}{V_{PTV}^{Ref}} \right]^{-1} * \left[\frac{O_{PTV-OAR}}{O_{PTV-OAR}^{Ref}} \right]^{-1} \quad (1)$$

where $NOS_{excluded}(\theta)$ is the number of segments excluded in a given BEV; θ characterizes the BEV in terms of a given combination of gantry, couch and collimator angles; V_{PTV} is the composite PTV volume in a given case; $NOS_{excluded}^{Ref}(\theta)$ is the number of segments excluded in a given BEV for a reference case; V_{PTV}^{Ref} is the composite PTV volume in the reference case; $O_{PTV-OAR}$ is the percentage of OAR overlap with the PTV (considering all OAR overlaps with PTV in BEV) in θ in a given case; $O_{PTV-OAR}^{Ref}$ is the percentage of OAR overlap with the PTV in θ in the reference case. In Table 1 we have attempted to model the segment reduction due to the BR process.

The maximum NOS obtained for each beam by applying the above processes (Sections 3.2.1–3.2.4) will be summed up and fed into the DMPO module, which will determine the final deliverable segments and thus the treatment plan accordingly. The whole process is modeled in Fig. 2.

4. Results

The proposed algorithm was tested in eight H&N cases. Our primary intention is to verify if the maximum NOS predicted using the AGSC method is appropriate in terms of plan quality and delivery efficiency. We first studied the impact of different maximum NOS settings on the plan quality ranging from 10 to 100. Independently, we employed the maximum NOS predicted by the AGSC method for the same cases and compared the results.

For all plans, an equispaced beam configuration was created with seven beams (H&N cases 1–5) and nine beams (H&N cases 6–10). Auto Plan feature¹⁵ available in Pinnacle (Version 9.10.0) was used to drive the optimization process

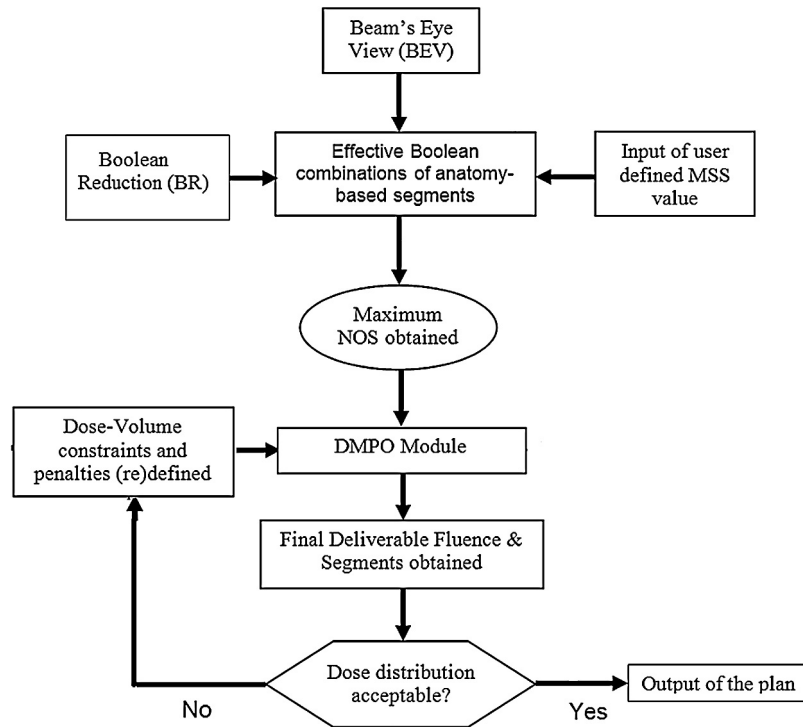


Fig. 2 – The flow chart of anatomy-guided segment counting (AGSC) algorithm.

Table 2 – Dose-volume objectives specified for all Head and Neck cases used in the study. Total number of fractions was 35 in all the cases.

Organ	Objective type	Dose (cGy)	Volume (%)
PTV 7000	Target Dose	7000	95
PTV 6300	Target Dose	6300	95
PTV 5600	Target Dose	5600	95
Spinal cord	Max Dose	4500	0
Brain stem	Max Dose	5400	0
Larynx	Mean Dose	5000	NA
Parotids	Mean Dose	2600	NA
Lips	Mean Dose	3500	NA
Oral cavity	Mean Dose	3800	NA
Esophagus	Max DVH	3500	50
Mandible	Max Dose	7000	0
Submandibular	Mean Dose	4000	NA

automatically. For all plans, 4 MU and 6 cm² were set as the minimum MU and minimum segment size (MSS) constraints, respectively. The MSS of 6 cm² is input into both the AGSC method as well DMPO optimization. The composite target volume (the geometric sum of all PTVs) in the plan is considered for segment counting. Also the critical OARs – the spinal cord, brainstem, parotids (right and left) – only were considered for the segment counting process. Table 2 gives D-V objectives specified for all H&N cases used in the study. The plans created were used only for a simulation purpose and not delivered to any patients. The planning simulations were done using Varian Tx HDMLC machine.

Fig. 3 shows the graphical plot of how the composite objective value changes with respect to different maximum NOS

settings ranging from 10 to 100 for the eight H&N plans (H&N cases 1–8 represented by Fig. 3a–h, respectively).

The maximum NOS obtained from the AGSC method is also mapped on the same figure for all cases. In order to make composite objective value computation more clinically oriented, we only included the target volume and critical organ's objective values and excluded non-anatomical regions of interest (ROIs) created by Auto Plan module from objective value computation. Fig. 4 shows the DVH comparison at different NOS per beam specifications including AGSC-based specification for a sample case (H&N 1) involving seven beams. Table 3 shows the comparison of the final number of segments obtained in different maximum NOS per beam specifications including AGSC-based specification. Table 4 shows the comparison of composite objective value and total MUs obtained in different maximum NOS per beam specifications including AGSC-based specification. Table 5 shows how the input of different Minimum Segment Size (MSS) values into the AGSC module impacts the plan quality and the maximum NOS resulting from the AGSC algorithm.

As a part of the experiment, we asked an experienced clinical user to choose an appropriate maximum NOS per beam for the same H&N cases without disclosing the results from the AGSC method. The clinical user's decision was to use 8 NOS per beam for all H&N cases. Fig. 5 shows the DVH comparison between user-selected 8 NOS per beam plan and AGSC plan for sample H&N cases (H&N case 1 and 4) involving seven and nine beams respectively. Fig. 6 shows the DVH comparison between user-selected 8 NOS per beam plan and AGSC plan for sample H&N cases (H&N case 2 and 5) involving seven and nine beams, respectively.

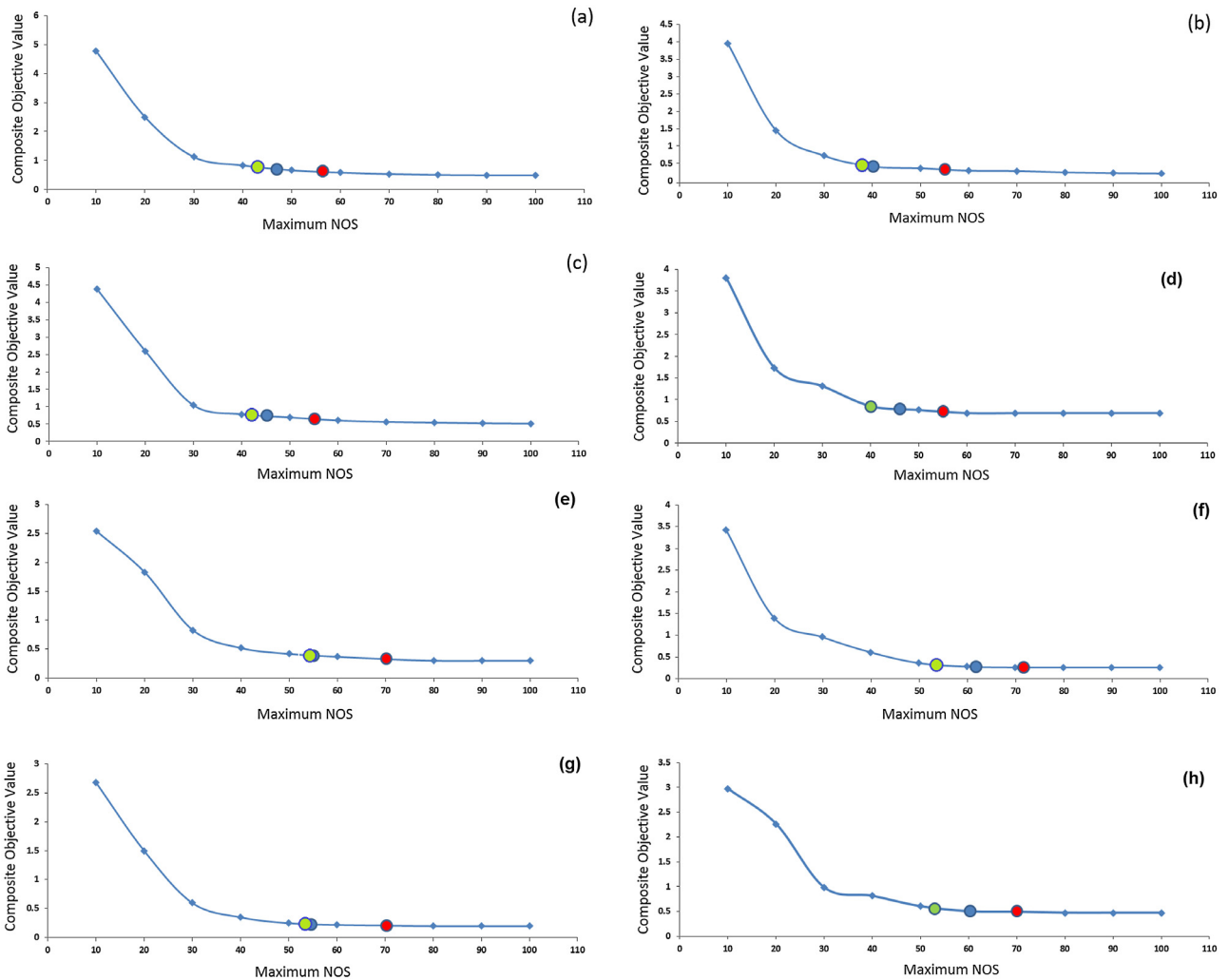


Fig. 3 – Graphical plot of how the composite objective value changes with respect to different maximum NOS setting ranging from 10 to 100 for the ten H&N plans (H&N cases 1–8 represented by (a)–(h), respectively). Here green, red and blue circles denote the composite objective values corresponding to the plans employing 6 NOS per beam, 8 NOS per beam and AGSC-predicted NOS per beam, respectively.

It is evident from Fig. 3 that the plan quality starts diminishing when the specified maximum NOS per beam approximately reaches a lower bound of 6. Also the plan quality is saturated (i.e. no further improvement in plan quality is produced) when the specified maximum NOS per beam approximately reaches an upper bound of 8. Green, red and

blue circles in Fig. 3 denote the composite objective values corresponding to the plans employing 6 NOS per beam, 8 NOS per beam and AGSC-predicted NOS per beam, respectively. It is evident from Fig. 3 that the maximum NOS per beam predicted by AGSC method arrives in between 6 and 8 for all eight H&N cases.

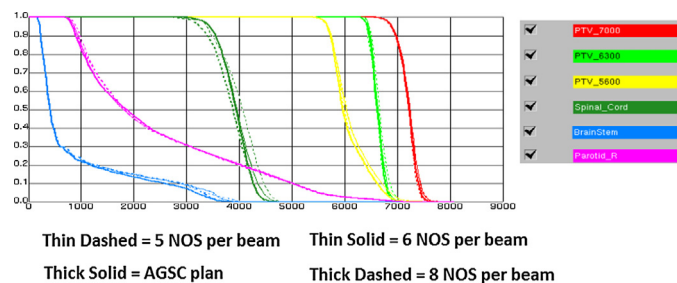


Fig. 4 – DVH comparison at different NOS per beam specifications including AGSC-based specification for a sample case (H&N 1) involving seven beams.

Table 3 – Comparison of the number of segments specified and obtained in (a) 6 NOS per beam specification, (b) 8 NOS per beam specification, and (c) AGSC-based specification. The numbers in square brackets are the number of segments removed from the Boolean reduction process.

Study case	Total number of beams	Maximum NOS specified (obtained) – 6 NOS	Maximum NOS specified (obtained) – 8 NOS	Maximum NOS specified (obtained) AGSC method
H&N 1	7	42 (42)	56 (56)	50 (48)[6]
H&N 2	7	42 (38)	56 (56)	44 (40)[12]
H&N 3	7	42 (41)	56 (55)	45 (45)[7]
H&N 4	7	42 (40)	56 (56)	46 (46)[6]
H&N 5	9	54 (54)	72 (71)	56 (56)[9]
H&N 6	9	54 (54)	72 (72)	62 (62)[6]
H&N 7	9	54 (53)	72 (71)	58 (55)[7]
H&N 8	9	54 (53)	72 (70)	62 (60)[3]

Table 4 – Comparison of final objective function and total MU obtained in (a) 6 NOS per beam specification, (b) 8 NOS per beam specification, and (c) AGSC-based specification.

Study case	Final composite objective value			Total MU		
	6 NOS	8 NOS	AGSC-method	6 NOS	8 NOS	AGSC-method
H&N 1	0.7311	0.5947	0.6729	601	705	619
H&N 2	0.4293	0.3195	0.3828	654	728	667
H&N 3	0.8164	0.6106	0.6573	554	616	578
H&N 4	0.1945	0.1751	0.1724	559	597	571
H&N 5	0.3779	0.3012	0.3451	620	798	665
H&N 6	0.2964	0.2147	0.2413	750	859	780
H&N 7	0.2215	0.2101	0.1985	640	806	673
H&N 8	0.1501	0.1285	0.1362	613	715	664

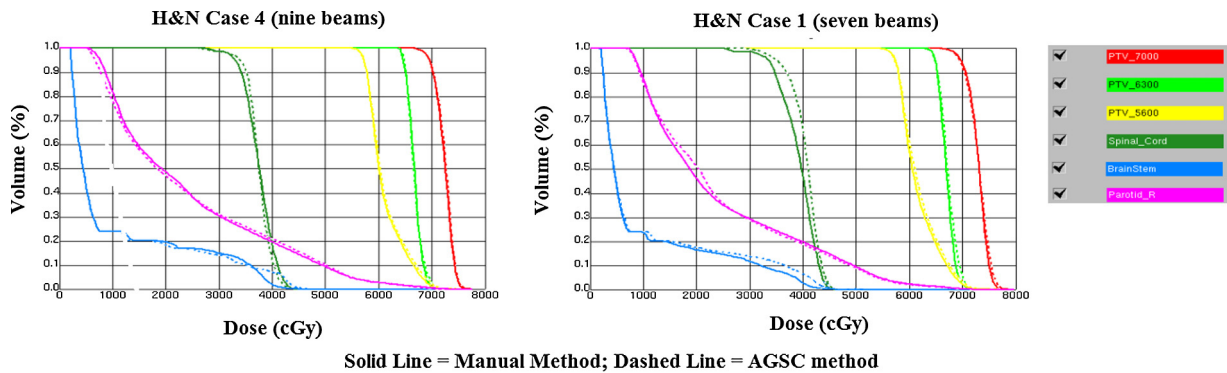


Fig. 5 – DVH comparison of user-selected 8 NOS per beam plan and AGSC plan for sample H&N cases (H&N case 1 and 4) involving seven and nine beams, respectively.

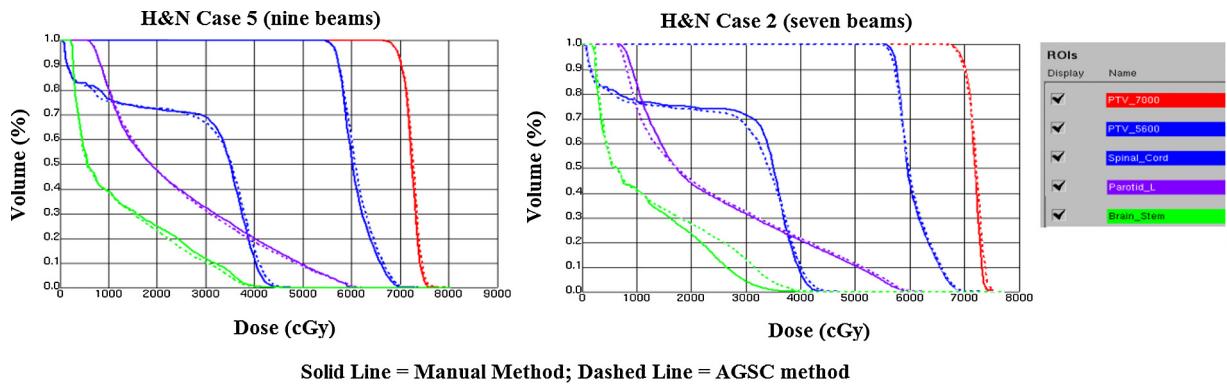


Fig. 6 – DVH comparison of user-selected 8 NOS per beam plan and AGSC plan for sample H&N cases (H&N case 2 and 5) involving seven and nine beams, respectively.

Table 5 – The change in maximum NOS and composite objective value when different minimum segment size (MSS) value is input into the AGSC algorithm for H&N 1 involving seven beams.

MSS (cm ²)	Maximum NOS obtained from AGSC method and specified into DMPO	NOS obtained after final DMPO optimization	Composite objective value
2	52	52	0.6318
4	50	50	0.6375
6	50	48	0.6729
8	46	45	0.6778
12	39	38	0.6883
16	37	36	0.6951
20	34	34	0.7404

On the plan quality front, there is about 13% reduction in the composite objective value (on the average) in AGSC plans as compared to the plans employing 6 NOS per beam and 10% increase in the composite objective value (on the average) in AGSC plans as compared to the plans employing 8 NOS per beam. Moreover, Fig. 4 (DVH comparison) indicates that the plan quality diminishes below a maximum NOS per beam setting of 6. Especially the spinal cord dose keeps increasing as the maximum NOS per beam is reduced (Spinal cord Max dose at: 8 NOS per beam = 46 Gy; AGSC-based NOS per beam = 46 Gy; 6 NOS per beam = 48 Gy; 5 NOS per beam = 50 Gy). On the delivery efficiency front, there is about 10% increase in NOS and 5% increase in total MU (on the average) in AGSC plans as compared to the plans employing 6 NOS per beam specification. Similarly, there is about 19% reduction in NOS and 10% reduction in total MU (on the average) for AGSC plans as compared to the plans employing 8 NOS per beam specification.

Figs. 5 and 6 are indicative of equivalent plan quality of plans employing user-selected maximum NOS per beam and AGSC-based NOS per beam. These results indicate that AGSC approach could strike a good balance between plan quality (i.e. lower composite value) and delivery efficiency (i.e. reasonably lower number of segments) accounting for the complexity of a given case.

There are studies that have shown that generating segments based on the anatomy coupled with a segment weight optimization can produce IMRT equivalent treatment plans with improved delivery efficiency.^{16–18} These approaches are collectively regarded as “Anatomy-based Inverse Planning (ABIP)”. In fact, the direct aperture optimization techniques in the current form of are some kind of variants of the ABIP technique. Our present work shows that the incorporation of anatomic and geometric elements into DMPO optimization is still useful for creating better and efficient treatment plans.

The proposed method accounts for various case-specific parameters such as PTV-OAR geometry, PTV size (by means of BR process), number of beams, beam angles and user-defined MSS value. Hence, one can expect a clinically relevant solution from the AGSC approach. Initially, we considered the number of PTVs for the counting process for simultaneously integrated boost (SIB) cases and we found that it generally produced more than sufficient NOS. So we recommend not

to explicitly consider the number of PTVs intersecting a given BEV for the counting process, rather just consider the composite PTV. However, the proposed method allows including the number of PTVs for the counting process by considering them as regions of interest in the similar manner to how we consider the OARs.

Auto Plan has been used just as a substitute to an expert planner in this study. In the absence of Auto Plan feature, a planner has to manually tweak the objective function parameters before starting the optimization in order to meet the clinical objectives when the maximum NOS is increased or decreased. It is to be noted that the method relies on the user-defined number of beams and beam angles.

It is to be noted that the proposed AGSC method relies on the user-defined number of beams for determining the number of segments. When using the AGSC method in DMPO, an incorrect selection of beam number can result in incorrect specification of maximum number of segments. Recently, we proposed a method to optimize the number of beams in DMPO-based IMRT.¹⁹ By integrating the AGSC method with such beam number determination methods, it is possible to maximize the potential of the proposed method for determining optimal number of segments.

5. Conclusion

In this paper, we introduced an empirical method for automatic and case-specific selection of maximum NOS for DMPO-based IMRT. Our attempt was to integrate the basic elements of Anatomy-based IMRT into the DMPO process. Our investigation shows that the AGSC method allows specifying suitable number of segments into the DMPO module. Though we used H&N anatomy to demonstrate the algorithm in this study, in theory, the algorithm will also be applicable to other anatomies such as the pelvis and thorax.

Conflict of interest

None declared.

Financial disclosure

None declared.

REFERENCES

- Cotrutz C, Xing L. Segment-based dose optimization using a genetic algorithm. *Phys Med Biol* 2003;48:2987–98.
- Siebers JV, Lauterbach M, Keall PJ, Mohan R. Incorporating multi-leaf collimator leaf sequencing into iterative IMRT optimization. *Med Phys* 2002;29:952–9.
- Nadeau S, Bouchard M, Germain I, et al. Postoperative irradiation of gynecologic malignancies: improving treatment delivery using aperture-based intensity-modulated radiotherapy. *Int J Radiat Oncol Biol Phys* 2007;68:601–11.
- Hårdemark B, Liander A, Reh binder H, Löf J. Direct machine parameter optimization with RayMachine® in Pinnacle3®. *RaySearch White Paper*. Stockholm, Sweden: RaySearch Laboratories AB; 2003.

5. Carlsson F. Combining segment generation with direct step-and-shoot optimization in intensity-modulated radiation therapy. *Med Phys* 2008;**35**:3828–38.
6. Dobler B, Pohl F, Bogner L, Koelbl O. Comparison of direct machine parameter optimization versus fluence optimization with sequential sequencing in IMRT of hypopharyngeal carcinoma. *Radiat Oncol* 2007;**6**:33.
7. Dobler B, Koelbl O, Bogner L, Pohl F. Direct machine parameter optimization for intensity modulated radiation therapy (IMRT) of oropharyngeal cancer – a planning study. *J Appl Clin Med Phys* 2009;**10**:3066.
8. Ludlum E, Xia P. Comparison of IMRT planning with two-step and one-step optimization: a way to simplify IMRT. *Phys Med Biol* 2008;**53**:807–21.
9. Jones S, Williams M. Clinical evaluation of direct aperture optimization when applied to head-and-neck IMRT. *Med Dosim* 2008;**33**:86–92.
10. Worthy D, Wu Q. Parameter optimization in HN-IMRT for Elekta linacs. *J Appl Clin Med Phys* 2009;**10**:43–61.
11. Jiang Z, Earl MA, Zhang GW, Yu CX, Shepard DM. An examination of the number of required apertures for step-and-shoot IMRT. *Phys Med Biol* 2005;**50**:5653.
12. Cheong K-H, Kang S-K, Lee MY, et al. Analytic study on the effects of the number of MLC segments and the least segment area on step-and-shoot head-and-neck IMRT planning using direct machine parameter optimization. *J Korean Phys Soc* 2013;**62**:1330–9.
13. Qi P, Xia P. Relationship of segment area and monitor unit efficiency in aperture-based IMRT optimization. *J Appl Clin Med Phys* 2013;**14**:232–43.
14. Ranganathan V, Ranjan US. Apparatus for determining a number of beams in IMRT. United States patent application, 2014; US14/763539.
15. Hazell I, Bzdusek K, Kumar P, et al. Automatic planning of head and neck treatment plans. *J Appl Clin Med Phys* 2016;**17**:272–82.
16. De Gersem W, Claus F, De Wagter C, De Neve W. An anatomy-based beam segmentation tool for intensity-modulated radiation therapy and its application to head-and-neck cancer. *Int J Radiat Oncol Biol Phys* 2001;**51**:849–59.
17. Beaulieu F, Beaulieu L, Tremblay D, Lachance B, Roy R. Automatic generation of anatomy-based MLC fields in aperture-based IMRT. *Med Phys* 2004;**31**:1539–45.
18. Ranganathan V, Narayanan VS, Bhangle JR, et al. Performance evaluation of an algorithm for fast optimization of beam weights in anatomy-based intensity modulated radiotherapy. *J Med Phys* 2010;**35**:104–12.
19. Ranganathan V, Das KM. Determination of optimal number of beams in direct machine parameter optimization-based intensity modulated radiotherapy for head and neck cases. *J Med Phys* 2016;**41**:129–34.